INNOVATIVE AIRCRAFT AEROELASTIC MODELLING & CONTROL

M.Battipede, E.Cestino, G.Frulla, S. Gerussi, P.Gili
Department of Aerospace Engineering, Politecnico di Torino, Italy.

Abstract

The aeroelastic design of innovative aircraft wing configurations imposes the designer to deal with specific phenomena, which are not usually considered in classical aircraft definition. The design process itself, though, gives the designer several indications on how to maintain the safety standards imposed by regulations. The investigation of the basic aeroelastic principles for unconventional wings with high aspect ratios can be extremely interesting as, once introduced in a multidisciplinary design, they can be very effective in giving an early determination of the static and dynamic behaviour of the aircraft, leading to significant improvements in the configuration weight, cost, and overall performance. The paper shows some preliminary results as part of the main objectives of the In.A.Team group (Innovative Aircraft Theoretical-Experimental Aeroelastic Modelling) at Politecnico di Torino, Italy. The ***In.A.Team*** *Project has the following main objectives:*

- *to develop multidisciplinary analysis methods appropriate to unconventional aircrafts (highly flexible, "morphing" vehicles);*
- *to develop the capability of illustrating and understanding the effects of uncertainties on the behaviour of an aeroelastic system;*
- *to apply the innovative adaptive $\mathcal{L}_1$ control techniques to highly flexible wings,*
- *to integrate theoretical analysis with commercial structural (FEM) and aerodynamic tools (CFD).*
- *to design and manufacture an aeroelastic experimental-test-model.*
- *to validate theoretical/numerical results by vibration and aeroelastic wind tunnel tests.*

1 Introduction

Innovative aircraft wings such as High-altitude, long-endurance (HALE) aircraft employ slender, flexible wings to reduce weight and enable the high lift-to-drag ratios necessary to achieve sustained flight for months or years. Increased wing flexibility can lead to large static structural deflections for trimmed states, which has attracted researchers to the effects of geometric nonlinearity on the flight dynamics [1,2] and dynamic stability [3,4,5] of standard unswept wings or more advanced joined-wing vehicle concepts [6].

The complete nonlinear-aeroelastic analysis is extremely complex and requires an integration of different disciplines to develop a new design approach, effective in forecasting and avoiding catastrophic events such as the one occurred to the NASA's Helios aircraft. The Helios Prototype aircraft involved in the mishap was a proof-of-concept solar electric- powered flying wing designed to perform high altitudes high endurance missions. The failure occurred during a test flight on June 26, 2003. The NASA Mishap Investigation indicated that the Helios Prototype appeared to have experienced undamped pitch oscillations that had led to a partial breakup of the aircraft. Following the episode, main NASA recommendations were

revised as to include: 1) the development of more advanced, multidisciplinary "time-domain" analysis methods appropriate to highly flexible, "morphing" vehicles; 2) the development of ground-test procedures and techniques appropriate to this class of vehicles to validate new analysis methods and predictions; 3) the development of multidisciplinary models, which can describe the nonlinear dynamic behaviour of aircraft modifications [7].

The In.A.TEAM Project has a theoretical/experimental nature and the main scope is the investigation of basic aeroelastic principles for unconventional high aspect ratio wings. The main objective is to develop simple analytical methods which should be used for a better understanding and estimation of the main factors contributing to the occurrence of different critical and supercritical behaviour of such an aircraft. Early determination of the static and dynamic behaviour of an aircraft can lead to significant improvement in configuration weight, cost, and performance. In the preliminary design phase, analytical methods are preferred when included into the integrated design process. Aeroelastic critical velocities estimated from deterministic analyses, assume that physical and geometrical parameters are perfectly known. However, deterministic mechanical description of composite material may be too penalizing, leading to an increase in structures weight, or may be not conservative, leading to unacceptable safety levels.

Accuracy of the simple analytical structural models must be adequate to develop and design active control systems for the suppression of aeroelastic oscillations, which might lead to critical instability phenomena. It is very well known that the employment of adaptive active control technique is extremely relevant on high aspect ratio wings. As a matter of fact, active control improves structural response, without the added weight penalty, as opposed to passive control, where increasing in structural rigidity is achieved at the weight expenses. Active control can take advantage of the technological developments in the areas of materials and computer sciences. The combination of multifunctional materials with faster computers and real time data acquisition systems has paved the way for the application of adaptive control techniques, able to mitigate structural problems and robust to uncertainties, noise and highly variable external loads. In particular, among the adaptive active control system, the $\mathcal{L}_1$technique has shown interesting features: the investigation of possible application to flutter control for high aspect ratio composite wings is exactly one of the topics of the In.A.TEAM Project.

This paper presents a preliminary analysis of an advanced control strategy architecture which will be the basis for future development. In particular, section 2 presents a brief survey of the aeroelastic models which can be developed for flutter prediction and control. In section 3, a simple 3 degree-of-freedom (DOF), bidimensional wing model is then developed and validated with results collected in the present literature. A motivational example is shown on the Goland's wing in Section 4: the limits of an output feedback linear quadratic regulator (LQR) control strategy are analyzed, especially in presence of gradually or instantaneous degradation of the structural bending stiffness. Finally, the mathematical implications of the $\mathcal{L}_1$ control technique are discussed.

2 Aeroelastic models

This section discusses a range of structural models for aeroelastic analysis with the purpose of determining the level of physical fidelity to predict the flutter boundary of a composite high aspect ratio wing configuration. The simplest model of an aeroelastic system with bending torsion instability is the classical typical airfoil section model based on linear springs (Fig. 1), which can be considered the first term of comparison [8]. It is essentially an elastic structure constrained in the pitch (ϕ) and plunge, (h). Despite its simplicity, it continues to be a test bed for investigations of nonlinear stiffness [9], flutter and limit cycle oscillations, dynamic stall [10] as well as structural uncertainty effect on classical wing flutter characteristics [11].

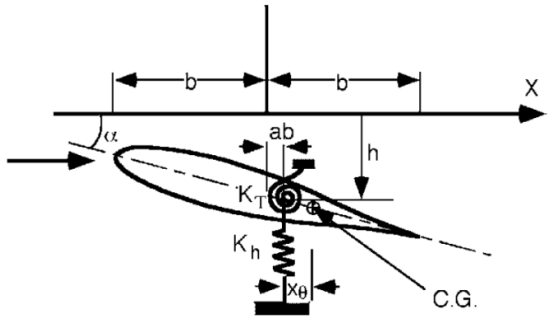

Fig 1. Typical airfoil section model.

A more realistic wing model for composite structures can be obtained introducing a bending-torsion coupled stiffness K by using a wing-box model for the wing cross-section and a circumferentially asymmetric stiffness (CAS) configuration for the composite ply lay-up. The resultant equations of motion can be expressed in nondimensional form as follows:

$$\begin{bmatrix} 1 & \bar{x}_\alpha \\ \bar{x}_\alpha & \bar{r}_\alpha^2 \end{bmatrix} \begin{Bmatrix} \ddot{w} \\ \ddot{\phi} \end{Bmatrix} + \begin{bmatrix} c_{11}\frac{\Theta \bar{r}_\alpha^2}{\lambda^2} & c_{12}\frac{\bar{K}\bar{r}_\alpha^2}{\lambda} \\ c_{21}\frac{\bar{K}\bar{r}_\alpha^2}{\lambda} & c_{22}\bar{r}_\alpha^2 \end{bmatrix} \begin{Bmatrix} w \\ \phi \end{Bmatrix} = = \begin{Bmatrix} -\frac{1}{\mu} C_L(\hat{t}, a, k^*) \\ \frac{2}{\mu} C_M(\hat{t}, a, k^*) \end{Bmatrix} \quad (1)$$

where:

$$k^* = \frac{\omega_r \cdot b}{U}; \quad \lambda = \frac{L}{b}; \quad \mu = \frac{m}{\pi \rho b^2};$$
$$\bar{K} = \frac{K}{G \cdot J_t}; \quad \Theta = \frac{E \cdot I}{G \cdot J_t}; \quad \bar{X}_\alpha = \frac{e}{b}; \quad (2)$$
$$\bar{r}_\alpha = \frac{r_\alpha}{b}$$

and c_{11},c_{12},c_{22} are coefficients dependent on the shape functions used for the 2 D.o.F. reduction. Lift and moment coefficients are determined through an external unsteady aerodynamic model. Generally speaking, the models used for the calculation of unsteady aerodynamic loads can be divided into three groups:

- analytical models such as Theodorsen's function, Wagner's function, Kussner's function, strip theory, piston theory etc.
- models based on the Euler/Navier-Stokes equations, which might be extremely demanding as far as computing resources are concerned;
- models based on singularity elements such as vortex-lattice methods or vortex-panel methods.

During the preliminary design phase, when parametrical studies and comparisons of different configurations have to be performed, a time-saving procedure can be of strategic importance. For this reason analytical models are usually favoured at this stage, especially if expressed in the state-space formulation, particularly useful for control applications. Wagner's function or Roger's approximation are thus preferred as they accurately transforms the unsteady aerodynamic forces from frequency to time domain.

It is important to noticed that, when the values of the angle-of-attack become significant, the aerodynamic nonlinearities could play an important role in the critical and post-critical aeroelastic behaviour, modifying consistently the flutter characteristics. To take into account this effect, semi-empirical dynamic stall models can be introduced. The current literature presents a variety of different empirical models of dynamic stall: for example there is the model developed at the ONERA research center [10] or the Beddoes [12] model, later extended by Leishman and Beddoes [13], among the others. The aerodynamic model considered in this paper omits the stall model, which limits the analysis to a basic flutter prediction.

The more complex model of Fig. 2 can be obtained using a set of nonlinear beam equations, which highlight the bending-torsion elastic coupling due to two different effects:

- the composite coupling due to the CAS configuration;
- the coupling deriving from the second-order geometric non-linearities.

Removing these nonlinearities the model reduces to the classical Euler-Bernoulli composite beam equations, which enables the investigation of structural nonlinear effects on flutter and limit cycle oscillations.

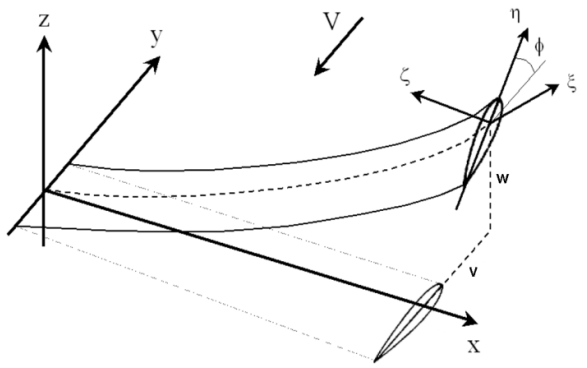

Fig 2. Non linear composite Euler-Bernoulli beam model

The governing aeroelastic equations are derived, in the case of a nonlinear and initially straight and inextensional composite Euler-Bernoulli beam model, using the extended Hamilton's principle [14,15,16,17]. The resulting equations are valid for long, slender, composite beams, experiencing displacements from moderate to large (second-order approximation):

$$\begin{cases} m\ddot{v} + c_2\dot{v} + EI_3 v'''' + N_v = q \\ m\ddot{w} + c_3\dot{w} + me\ddot{\phi} + EI_2 w'''' - K\phi''' + N_w = q_w \\ j_1\ddot{\phi} + c_4\dot{\phi} + me\ddot{w} - GJ_t\phi'' + Kw''' + N_\phi = q_\phi \end{cases} \quad (3)$$

where N_v , N_w and N_ϕ are the second order non-linear terms:

$$\begin{aligned} N_v &= (EI_3 - EI_2)(w''\phi)'' + GJ_t(\phi w'')' + K(\phi''\phi)' \\ &\quad + K(\phi'\phi)' - K(w''w')' \\ N_w &= (EI_3 - EI_2)(w''\phi)'' - GJ_t\left(\phi' v''\right)' - K(v'''w')' \\ N_\phi &= (EI_3 - EI_2)(v''w'') - GJ_t(v''w')' + K(v'''\phi) \end{aligned} \quad (4)$$

The beam model considered in the present paper is derived under the same hypothesis discussed in [18,19] and can be considered adequate for preliminary parametric analysis of the flutter behaviour of slender wings. The general hypotheses is that the span-wise is by far greater than the transversal section dimension which, in turn, is greater than thickness. Under these assumptions, it is possible to adopt a beam-wise approximation to model the real wing-box/tubular main spar. The composite box was considered manufactured by planar and thin plate elements with different lay-ups, obtained assembling unidirectional or multidirectional composite plies. Assumptions on a constant shear flow and negligible circumferential stresses are applied in the derivation of the section stiffness. Strains are represented by longitudinal expression, according to the classical beam theory, whereas no indications are given concerning the displacements in the section plane. They are included in a mixed formulation where the shear flow is determined accordingly. Finally, stiffness expressions are defined and used for a preliminary structural approximation of the composite wing-box [18,19].

Flutter condition is, by definition, a borderline situation (or neutral stability) where disturbances may cause convergent or divergent oscillations, depending they occur in a range of speed below or above the flutter speed. The mathematical formulation leads to a complex eigenvalue problem, where two characteristic numbers have to be determined: speed and frequency. The flutter speed and frequency are defined as the lowest airspeed and corresponding frequency at which a given structure, flying in a specific atmosphere, will exhibit sustained simple harmonic oscillations.
What happens is that, in the flutter condition, the real part of at least one of the characteristic exponents changes its sign from negative to positive: zero damping parameter identifies flutter speed.
The classical flutter calculation [8] is derived following the well known *V-g* approach, which is referred to the undeformed configuration, considered as the initial steady state over which the small perturbations are superimposed. The dynamic characteristics of the perturbed motions do not depend on the specific steady condition assumed for their evaluation. Classical flutter speed or linear flutter speed (LFS) is usually calculated under this assumption. Conversely when the structure presents a non-linear behaviour, due to the high structural flexibility, the dynamic of the perturbed motion is influenced by the selected equilibrium point. The reduced linear perturbation system originates a linear approximation of the behaviour of the system in the neighbourhood of the static equilibrium point, with the possibility of calculating a flutter

speed for each trim condition. In this case the flutter speed is referred to as "flutter velocity in non-linear equilibrium condition" (NLFS). In the case of slender HALE structures the classical approach is no longer suitable to obtain correct flutter identification [3,4,5].

3 Flutter results on a simplified aeroelastic model

A preliminary analysis of the flutter dynamics, as well as a comparison between different control systems and actuation modes, is firstly carried out using a simplified, 2-dimensional, 3-degrees-of-freedom linear model (Fig.3).

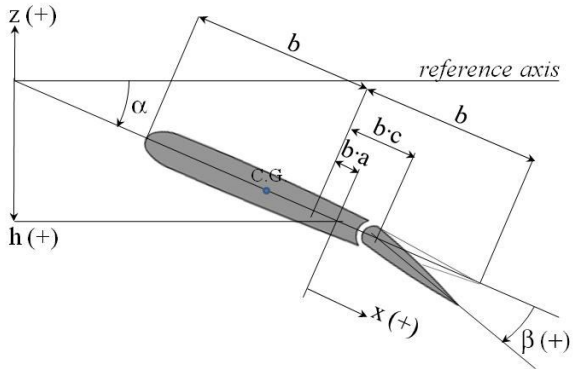

Fig 3. Simplified 3 D.o.F.

At this stage this is the only configuration taken into consideration, while further studies will extend the derived results to the 3-dimensional wing model to take into account the nonlinear effects (Fig.2).

The *V-g* method assumes harmonic motion at any given speed, under the hypothesis that the system is subject to an unknown artificial structural damping. Positive artificial damping is required for harmonic motion above flutter speed, while negative damping (i.e. excitation) is required below flutter speed to sustain the motion. Flutter speed is therefore defined as the speed at which the required artificial damping changes its sign.

Such an approach is well suited only for determining the flutter speed of a given model, rather than analyzing its dynamics and designing a control system. For this purpose, a state-space (SS) formulation which includes V as a parameter is necessary. To this purpose, Roger's approximation of the Theodorsen function [20] has been used to evaluate the aerodynamic forces in the time domain and obtain an SS-model by augmenting the system with additional states.

Under the assumption of small oscillations, and viewing the profile as a one-dimensional distribution of mass along the chord with density $\rho(x)$, we can write the vertical displacement z (positive upwards) of an arbitrary point of the profile as

$$z = -h - x\alpha - [x - b(c-a)]\beta \cdot U[x - b(c-a)] \quad (5)$$

where:

- h is the vertical displacement of the shear center (positive downwards)
- α is the airfoil angular deflection from the equilibrium condition (positive clockwise)
- x is the coordinate from the shear center along the chord (positive aft)
- b is the length of the half-chord
- a is the chordwise distance between the shear center and the midchord (nondimensional with b, positive with the shear center past the midchord)
- c is the chordwise distance between the trailing edge flap hinge and the midchord (nondimensional with b)
- β is the trailing edge flap deflection (positive clockwise)
- U is the unit step function centered on the trailing edge flap hinge.

The equations of motion can be derived using the Lagrange approach. The 3 degrees-of-freedom model can be thus described by the following equation:

$$\begin{cases} m\ddot{h} + S\ddot{\alpha} + S_\beta\ddot{\beta} + K_h h = F \\ S\ddot{h} + I\ddot{\alpha} + [I_\beta + S_\beta b(c-a)]\ddot{\beta} + K_\alpha\alpha = M_\alpha \\ S_\beta\ddot{h} + [I_\beta + S_\beta b(c-a)]\ddot{\alpha} + I_\beta\ddot{\beta} + K_\beta\beta = M_\beta \end{cases} \quad (6)$$

or in the equivalent matrix form, using nondimensional generalized forces and displacements:

$$\begin{bmatrix} m & \frac{S}{b} & \frac{S_\beta}{b} \\ \frac{S}{b} & \frac{I}{b^2} & \frac{I_\beta}{b^2}+\frac{S_\beta}{b}(c-a) \\ \frac{S_\beta}{b} & \frac{I_\beta}{b^2}+\frac{S_\beta}{b}(c-a) & \frac{I_\beta}{b^2} \end{bmatrix} \begin{Bmatrix} \frac{\ddot{h}}{b} \\ \ddot{\alpha} \\ \ddot{\beta} \end{Bmatrix} + \begin{bmatrix} \frac{K_h}{b} & 0 & 0 \\ 0 & \frac{K_\alpha}{b^2} & 0 \\ 0 & 0 & \frac{K_\beta}{b^2} \end{bmatrix} \begin{Bmatrix} \frac{h}{b} \\ \alpha \\ \beta \end{Bmatrix} = \begin{Bmatrix} \frac{F}{b} \\ \frac{M_\alpha}{b^2} \\ \frac{M_\beta}{b^2} \end{Bmatrix} \quad (7)$$

where:

- $K_{h,\alpha,\beta}$ are the linear springs restraining each degree of freedom. $K_{h,\alpha}$ model the flexural and torsional stiffnesses, while K_β models the stiffness of the flap mechanical link that restrains β to the commanded position β_c
- m is the section mass (including aileron)
- I is the section moment of inertia (including aileron) about the shear center
- S is the section static unbalance (including aileron) about the shear center (equal to mx_θ, x_θ being the distance between shear center and section CG, positive with the CG aft)
- I_β is the aileron moment of inertia about the hinge axis
- S_β is the aileron static unbalance about the hinge axis (equal to $m_\beta x_\beta$, m_β being the aileron mass and x_β being the distance between hinge axis and aileron CG, positive with the CG aft)

Forces and moments on the right-hand side of Eq. 7 are the unsteady aerodynamic forces and moments given by Roger's approximation [20]. Aerodynamic forces for the model of Fig.3 are expressed as:

$$\begin{Bmatrix} \frac{F}{b} \\ \frac{M_\alpha}{b^2} \\ \frac{M_\beta}{b^2} \end{Bmatrix} = q\left[2C(k)\{R\}[S_1]\{x_s\} + \frac{2b}{V}C(k)\{R\}[S_2]\{\dot{x}_s\} + \frac{2b^2}{V^2}[M_{nc}]\{\ddot{x}_s\} + \frac{2b}{V}[B_{nc}]\{\dot{x}_s\} + 2[K_{nc}]\{x_s\}\right] \quad (8)$$

where:

- $x_s = \begin{Bmatrix} h/b \\ \alpha \\ \beta \end{Bmatrix}$
- $C(k)$ is the Theodorsen function ([8])
- $k = \frac{\omega b}{V}$ is the reduced frequency of the section motion
- $q = \frac{1}{2}\rho V^2$ is the dynamic pressure
- $\{R\}, [S_1], [S_2], [M_{nc}], [B_{nc}], [K_{nc}]$ are quantities (derived from [21]) which depend only on the section geometry (through a and c).

As Theodorsen's theory is only valid for pure harmonic motion, it becomes less and less accurate as the real part of the dominant mode eigenvalue increases in absolute value. This is the reason why only the imaginary axis (and not whole s-plane) is considered when the least-square fit is performed to evaluate the approximated aerodynamic matrix from the exact one $A(s)$. This is also the reason why this model does not consider static divergence. The eigenvalues on the real axis (not plotted on the root loci in this paper) have nothing to do with static divergence: they refer to the augmented aerodynamic states and are always stable as long as the plunge and pitch flutter modes are stable.

Eq. 8 is written part in the frequency domain (the Theodorsen term) part in time domain (the state vector and its derivatives). Expressing the aerodynamic forces in the frequency domain only, Eq. 8 can be rewritten as:

$$\begin{Bmatrix} \frac{F}{b} \\ \frac{M_\alpha}{b^2} \\ \frac{M_\beta}{b^2} \end{Bmatrix} = q\left[2C(k)\{R\}[S_1] + 2s'C(k)\{R\}[S_2] + 2s'^2[M_{nc}] + 2s'[B_{nc}] + 2[K_{nc}]\right]\{x_s\} = qA(s')\{x_s\} \quad (9)$$

where $s' = s\frac{b}{V}$ is the nondimensional Laplace variable.

Roger's method approximates the exact aerodynamic matrix with the series:

$$A(s') \cong A_{ap}(s') = P_0 + P_1 s' + P_2 s'^2 + \sum_{j=3}^{N} \frac{P_j s'}{s' + \gamma_{j-2}} \tag{10}$$

where the γ_{j-2} are the aerodynamic poles, arbitrarily chosen in the range of reduced frequencies of interest. The coefficients of the matrices P_j are determined by performing least-square fit of the exact matrix $A(s')$ evaluated along the imaginary axis over M values of $s' = s\frac{b}{V} = i\omega\frac{b}{V} = ik$, with $M > N + 1$.

We define $N - 2$ augmented aerodynamic states as:

$$\{x_{aj}\} = \frac{s'}{s' + \gamma_{j-2}}\{x_s\} = \frac{s}{s + \frac{V}{b}\gamma_{j-2}}\{x_s\} \qquad j = [3 \dots N] \tag{11}$$

whose dynamics are by definition:

$$\{\dot{x}_{aj}\} = \{\dot{x}_s\} - \frac{V}{b}\gamma_{j-2}\{x_{aj}\} \tag{12}$$

Substituting Eq. 10 into Eq. 9 and comparing it to Eq. 8, the following expression can be obtained:

$$Ms^2\{x_s\} + K\{x_s\} = qP_0\{x_s\} + qP_1 s\frac{b}{V}\{x_s\} + qP_2 s^2\left(\frac{b}{V}\right)^2\{x_s\} + \sum_{j=3}^{N} qP_j\{x_{aj}\} \tag{13}$$

Performing the transformation from frequency to time domain, Eq. 13 and Eq. 12 can be rewritten together in matrix form as:

$$\begin{Bmatrix} \dot{x}_s \\ \ddot{x}_s \\ \dot{x}_{a3} \\ \dots \\ \dot{x}_{aN} \end{Bmatrix} = \begin{bmatrix} 0 & I & 0 & \dots & 0 \\ -\bar{M}^{-1}\bar{K} & -\bar{M}^{-1}\bar{B} & q\bar{M}^{-1}P_3 & \dots & q\bar{M}^{-1}P_N \\ 0 & I & -\frac{V}{b}\gamma_1 I & \dots & 0 \\ \dots & \dots & \dots & \dots & \dots \\ 0 & I & 0 & 0 & \frac{V}{b}\gamma_{j-2}I \end{bmatrix} \begin{Bmatrix} x_s \\ \dot{x}_s \\ x_{a3} \\ \dots \\ x_{aN} \end{Bmatrix} \tag{14}$$

where I is a $3x3$ identity matrix and

$$\bar{M} = M - qP_2\left(\frac{b}{V}\right)^2 \qquad \bar{B} = -qP_1\left(\frac{b}{V}\right) \qquad \bar{K} = K - qP_0 \tag{15}$$

The SS model is very effective in performing flutter predictions through the open loop root locus analysis and allows modern control techniques to be implemented as well. The obtained model has been validated by replicating the flutter parametric study of Ref. [8] (pp. 538-543). Fig.4 shows an example of a particular choice of system parameters from which it can be assumed that the two models are in a fairly good accordance. Discrepancies can be associated with the aerodynamic approximation (Eq. 10) introduced in the SS model of Eq. 14.

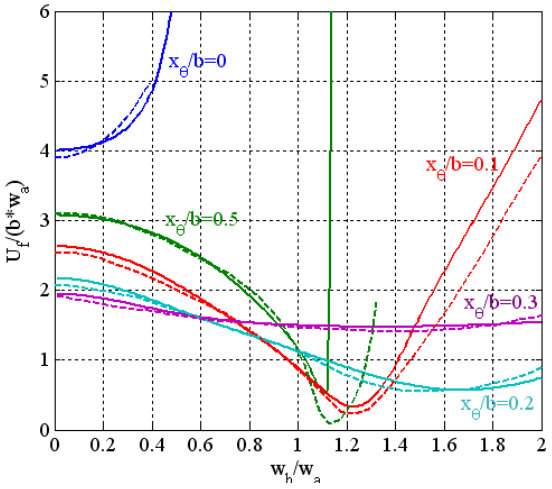

Fig.4. Comparison between the SS model with Roger's approximation (solid) and the model proposed in Ref. [8] (dashed)

4 Flutter Active Control

Goland's wing (Ref. [22]) has been selected as a test case for the problem of feedback control system design. It has been reduced to the 2-D case by considering per-unit-length inertial properties, and assuming linear spring rigidities such that the system's natural frequencies for the plunge and pitch mode are the same, respectively, of the first bending and first torsion modes of Goland's wing. Note that, so

far, only the A matrix of the SS model has been determined. While we can assume D to be null, and $C = [I^{6x6} \quad 0^{6x(3N-6)}]$ i.e. $y = [\{x_s\}^T, \{\dot{x}_s\}^T]^T$, the B matrix depends on the selected control actuation method. Two systems have been considered among those proposed in literature (Ref. [23-25]):

- the trailing edge flap;
- an array of piezoelectric patches applied to the wing surface to actively control its shape and rigidity.

The former is more conventional and of easier implementation, while the latter appears better suited for this kind of application mostly due to the bandwidth requirements.

From the point of view of the model of Fig.3, controlling the flap means applying an additional M_β, while controlling the wing shape through piezo patches means applying also the additional contribution F and M_α. In both cases it is more convenient to formulate the control problem as the tracking of the commanded signals $[h_c, \alpha_c, \beta_c]$ such that eq.(7) becomes:

$$M\begin{Bmatrix} \frac{h}{b} \\ \ddot{\alpha} \\ \ddot{\beta} \end{Bmatrix} + K\begin{Bmatrix} \frac{h-h_c}{b} \\ \alpha - \alpha_c \\ \beta - \beta_c \end{Bmatrix} = \begin{Bmatrix} \frac{F}{b} \\ \frac{M_\alpha}{b^2} \\ \frac{M_\beta}{b^2} \end{Bmatrix}_{aer} \tag{16}$$

It is now straightforward to derive a B matrix to write the system (14) in the SS form:

$$\begin{cases} \dot{x} = Ax + Bu \\ y = Cx + Du \end{cases}$$
$$x = \{x_s \quad \dot{x}_s \quad x_{a3} \quad \dots \quad x_{aN}\}^T \tag{17}$$
$$u = \left\{\frac{h_c}{b} \quad \alpha_c \quad \beta_c\right\}^T$$

Note that, even in the case of fully measurable $h, \dot{h}, \alpha, \dot{\alpha}, \beta, \dot{\beta}$, this is still an output feedback problem, due to the presence of the augmented aerodynamic states.

4.1 LQR control: motivational example

To control the Goland's wing through the deflection β_c of the trailing edge flap, an LQR output feedback has been designed. The open-loop root locus gives an additional proof for the validation of the model. Goland's wing, in fact, is supposed to flutter at $V_f \cong 137\ m/s$ (Fig.5), whereas the open-loop root locus gives $V_f \cong 139\ m/s$. Note that, however, the coupling of the flap dynamics with the plunge and pitch modes slightly reduces the flutter speed. This means that, under the hypothesis of an infinitely rigid trailing edge, the error between actual and calculated flutter speeds would be a little higher.

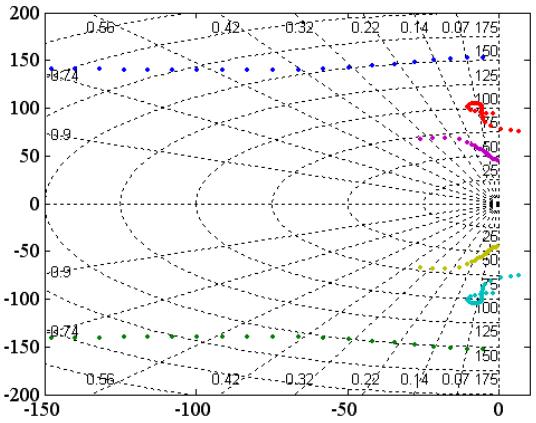

Fig.5. Goland's wing Open-Loop Root Locus

Setting the design airspeed at $V_d \cong 150\ m/s$, the LQR optimal gains are evaluated, stabilizing the system which would have otherwise never been able to reach the imposed design speed. The closed loop response of the Goland's wing to an impulse disturbance is shown in the simulation of Fig. 6.

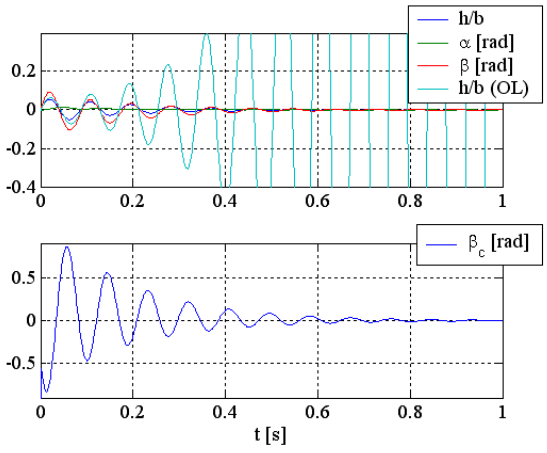

Fig.6. Goland's wing impulse response in Closed Loop

In what follows, robustness of this scheme is questioned. As shown by Bisplinghoff's parametric study mentioned earlier on, parameter variation can dramatically affect flutter speed. A parameter change might be

simple due to a gradual degradation of the material characteristics or to a sudden structure failure, which leads, for example, to a reduction of the structure stiffness. It must be said that, when a parameter change leads to the reduction of the flutter speed, usually the control activity necessary to damp the oscillations at the same design speed becomes much more demanding. When control saturation is an issue, hence, even perfect knowledge of the new parameters would not allow the design of a stabilizing controller. In order to show the lack of robustness of a fixed-gain LQR scheme and the importance of tailoring the control system to the actual system parameters, even when they do not affect flutter speed and do not require greater control authority, a motivational example is shown.

	Case A	**Case B**
$\omega_h\ [rad/s]$	98	56
$\omega_\alpha\ [rad/s]$	100	
$\omega_\beta\ [rad/s]$	300	
μ	20	
$x_\theta\ [m]$	0.3	
$r_\theta^2\ [m^2]$	0.25	
a	-0.4	
c	0.6	
$b\ [m]$	1	
$\rho\ [kg/m^3]$	1.225	
m_b/m	0.04	
S_b/S	0.0178	
I_b/I	0.002134	

Table 1. Parameter numerical values

Case A of Table 1 can be considered the baseline, with Case B being the very same configuration after a failure. Such would be the case of, say, a wingbox with reduced flexural stiffness, with no side effects on torsional stiffness and on the shear center position.
For both cases, the open-loop root loci are plotted with a maximum speed of $V_d \cong 230\ m/s$. As every dot of Fig. 7 and 8 correspond to a speed increment of *5m/s*, it is easy to deduce that both cases experienced flutter at $V_f \cong 215\ m/s$. The root loci and the open-loop eigenvalues are, however, dramatically different.

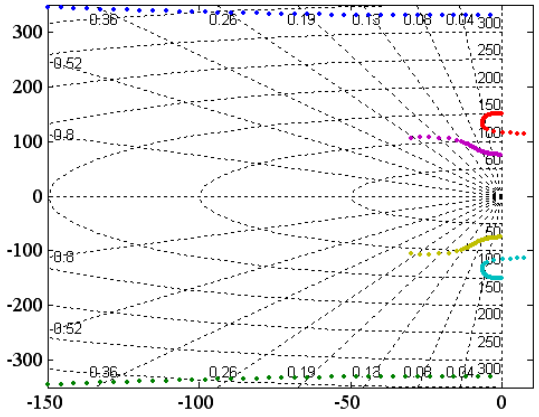

Fig.7. Case A Root Locus

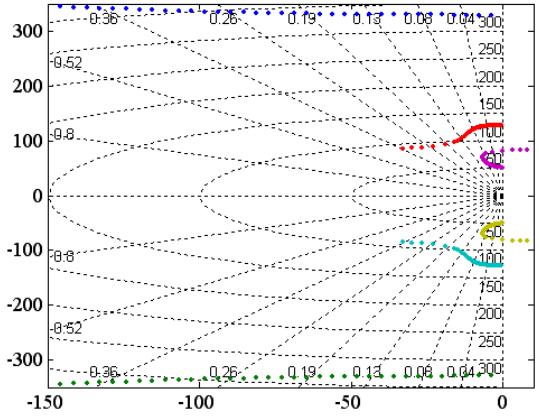

Fig.8 Case B Root Locus

For both cases an optimal LQR controller was designed. Fig. 9 and 10 show how stabilization is reached with a comparable control effort.

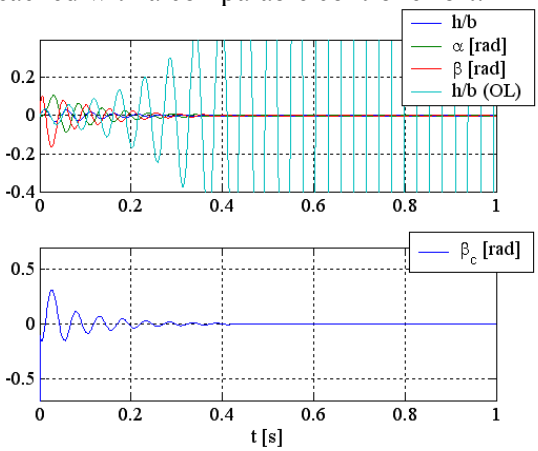

Fig.9. Case A CL impulse response
Gains K=[206.03 75.14 104.50 -4.71 -0.83 0.51]

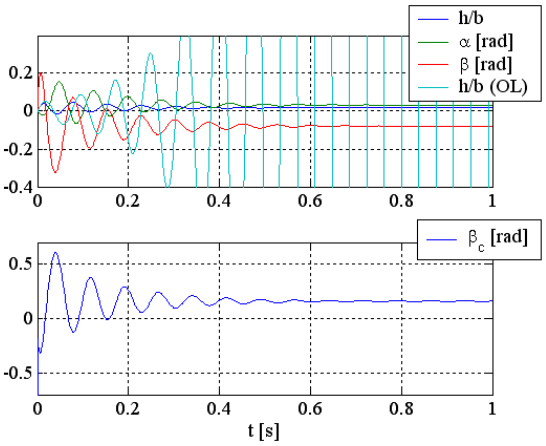

Fig.10. Case B CL impulse response
Gains K=[71.01 149.98 74.60 -4.98 0.15 0.37]

If, however, Case B is treated as a failure mode of Case A, and a simulation on the former is run using the controller for the latter, the closed-loop dynamics becomes marginally unstable, as shown in Fig. 11.

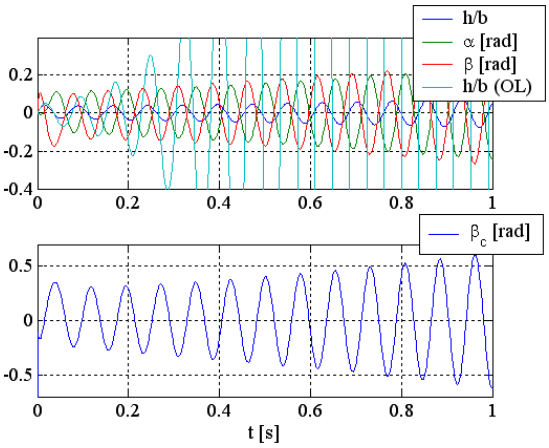

Fig.11: Case B CL impulse response
Gains K=[206.03 75.14 104.50 -4.71 -0.83 0.51]

The importance of parameter knowledge has been shown for this particular motivational example.

A more interesting situation, however, is the already mentioned more general case, where parameter variation does indeed lead to flutter speed change. It can be shown that, assuming that the new parameters were know, tailoring the control system to the updated conditions would lead to a higher closed loop flutter speed, under the same control authority. This implies, however, the employment of an adaptive control architecture, able to accommodate at least a given set of open loop dynamic modifications.

4.2 Adaptive Control architecture

Application of an adaptive controller was therefore investigated. In any adaptive architecture, feedback gains are neither fixed nor scheduled. A state-dependent adaptive law provides time-varying feedback gains $\hat{\theta}(x(t))$; the resulting control signal (being in the form $u(x) = \hat{\theta}^T(x) \cdot x$ is inherently nonlinear. Ideally, in the Model Reference Adaptive Controller (MRAC) subclass, the feedback gains should converge to their ideal value $\hat{\theta}^*$ so that the closed loop system replicates the dynamics of a given reference model (as shown in Fig. 12 for the Direct MRAC)

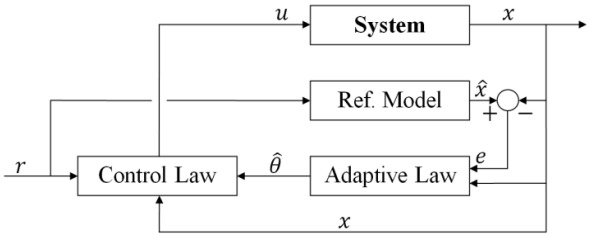

Fig.12. Direct MRAC

An issue typically left unaddressed by adaptive architectures is the tradeoff between adaptation and robustness. That is, fast convergence of the plant to the stable reference model can be easily achieved by selecting high adaptive gains in the adaptation law (note that these gains are a fixed design parameter). But, generally speaking, high adaptive gains can result in high frequency control signals, clearly unachievable by a real-world actuator due to its finite bandwidth, and arbitrarily bad transients (Ref. [26]), albeit asymptotic convergence is eventually achieved. On the other hand, selecting low adaptive gains allows for smoother control signals and transients, although tracking of the reference model is achieved only upon convergence of the feedback gains i.e. after a longer time, during which the system exhibits its own (unstable) dynamics.

Selection of a satisfactory value of the adaptive gains is a matter of trial-and-error tuning to each particular system.

The $\mathcal{L}_1$ class of MRAC controllers represents a recent development of the theory of adaptive control that circumvents this problem (Ref. [27-28]).

The key idea is to filter the control signal so that only achievable low-frequency signals are passed to the system, allowing higher adaptive gains to be adopted. The importance of this theory lies in the fact that it shows how the following objectives can be achieved by careful design of the lowpass filter :

- Boundedness of the control signal amplitude
- Boundedness of the tracking error

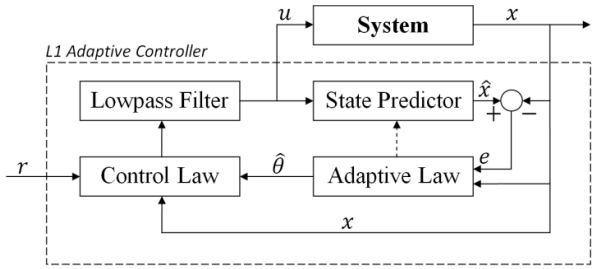

Fig.13. $\mathcal{L}_1$ Adaptive Controller Outline

Referring to of Fig.13, the *State Predictor* block, sometimes referred to as *Passive Identifier*, is in fact the stable reference system (whose state is $\hat{x}$) to be replicated by the closed-loop system (i.e., x must track $\hat{x}$). Indeed, its dynamics do contain the plant state multiplied by the estimated feedback gains (dashed connection) but if it were not for the *Lowpass Filter*, substitution of the *unfiltered* control signal would cancel those terms out from the Passive Identifier differential equation, leaving only the stable reference system tracking the input r with the assigned dynamics.

In the so-called *Passive Identifier based Reparameterization*, represented in Fig.14, both the plant and the reference system are fed with the same signal u (Fig.14), whereas in the dual case (i.e. *Direct MRAC* of Fig.12) the plant is fed with u while the reference system is directly fed with r.

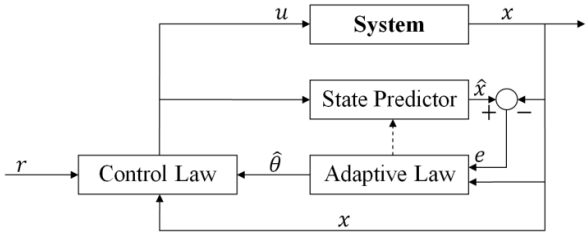

Fig. 14. Passive Identifier based reparameterization

In absence of the Lowpass Filter, the two schemes are perfectly equivalent under the same stability proof. Stability can be addressed in two steps:

- A Lyapunov-based stability proof for the tracking error between plant and reference system. This proof is not sufficient, though, as it only proves boundedness of the tracking error e, which could also occur with both systems drifting to infinity at the same rate. The adaptive law is defined at this stage.
- Convergence proof for the reference system (by definition, since it has arbitrarily assigned stable dynamics).

The only difference is that in the second scheme, it is only upon substitution of the control signal u that the Passive Identifier collapses to the Reference System, and stability follows.

In the $\mathcal{L}_1$ scheme of Fig.12, the presence of the Lowpass Filter makes things quite different. If the Direct MRAC scheme were used, in fact, only the plant input would have been filtered, adding states to the augmented plant-plus-filter system. Therefore x and $\hat{x}$ would not have the same dimension, e could not be defined and deriving a stabilizing adaptive law via a Lyapunov proof would be no longer possible.

It is hence clear that the implementation of the Lowpass Filter forces the use of the Passive Identifier scheme. Since both the plant and the Passive Identifier are fed with the same control signal, u cancels out in the error dynamics and the first step in the stability proof is left unchanged, regardless of the filtering.

On the contrary, the second step takes a different approach. Filtering of the control signal means that inside the State Predictor

block, cancelation of the feedback gain and plant state terms does no longer take place. Stability of the Predictor can still be proven with the Small-Gain theorem (Ref. [29]), given that the Lowpass Filter satisfies certain necessary conditions stated during the proof.

The aforementioned $\mathcal{L}_\infty$-norm bounds are also derived: they depend on the $\mathcal{L}_1$-norm of certain transfer function defined inside the closed-loop system, hence the name of the control architecture. The $\mathcal{L}_1$-norm of a transfer function is also known as the $\mathcal{L}_\infty/\mathcal{L}_\infty$-induced norm of the system.

It should be noticed that, apart from the capability of self-adjusting to unknown system parameters, $\mathcal{L}_1$ controllers (just as any other adaptive controller implementing projection-based adaptation) display another extremely useful feature, that is the disturbance rejection capability, which results in the boundedness of tracking error, even under the action of external disturbances, e.g. gust or signal noise.

At the current stage of the *In.A.Team* project, application of the $\mathcal{L}_1$ architecture to the active stabilization of a wing subject to aeroelastic phenomena is still under investigation, even for the simplest case of the 2-D model previously discussed. Nevertheless, some words can be spent on the characterization of the problem. As it was mentioned earlier on, in fact, all MRAC schemes involve the arbitrary choice of a stable reference model defined via its Hurwitz state matrix A_m. The whole subsequent theory relies on the assumption that there exists an ideal feedback gain matrix (for a scalar control signal, the vector θ^* mentioned earlier on) such that the closed loop system replicates the reference model. If the plant were known, it would be easy to determine θ^*. Adaptive control, though, is required precisely to deal with the plant uncertainties. Knowledge of θ^*, anyway, is not required; otherwise, there would be no need for an adaptive law. Only its existence is assumed, a condition trivially satisfied in the case of scalar x. In all other cases, the so-called *matching assumption* is formulated. That is, given the open-loop system:

$$\dot{x}(t) = Ax(t) + bu(t) \tag{18}$$

and a reference model

$$\dot{x}_m(t) = A_m x_m(t) + b_m r(t) \tag{19}$$

then there exists a feedback control signal:

$$u(t) = \theta_x^* x(t) + \theta_r^* r(t) \tag{20}$$

such that the original system of Eq.(18) mimics the reference model of Eq. (19). That is,

$$\begin{aligned} \exists\, \theta_x^*: &\quad A + b\theta_x^* = A_m \\ \exists\, \theta_r^*: &\quad b\theta_r^* = b_m \end{aligned} \tag{21}$$

In a nutshell, the matching assumptions require that the uncertainties are factored by the system's control matrix b. The uncertainties are defined in terms of the difference between the actual system matrices and the reference model matrices – but since the former is unknown, the latter cannot be chosen in order to satisfy Eq. (21).

Unless the control actuation method is such that b can factor any uncertainty, the matching assumptions are typically not satisfied by a real-world dynamic system.

The previously discussed 2-D, 3-Degrees-of-freedom flutter model featuring the trailing edge flap as the only effector represents an *unmatched uncertainties* problem. If the flap is removed (2-DoF left) and actuation is achieved through an array of piezo patches layered as to independently control both bending and torsion, the resulting system falls back into the *matched uncertainties* class of problems and can be solved with the current theory. As in a typical wing, trailing edge control surfaces are however present, the third degree of freedom cannot usually be removed from the model. Interlacing the $\mathcal{L}_1$ flutter control system with the flight control system to use both the piezo patches array and the flap as actuators might be required if the system has to be treated as a matched uncertainty problem.

The latest developments in $\mathcal{L}_1$ control theory (Ref. [30]) allow solution of the unmatched uncertainties case too, even though the adaptive laws used are derived in a different way. An $\mathcal{L}_1$ adaptive controller for systems with unmatched uncertainties with classic gradient-based

adaptive laws derived through conventional Lyapunov design is currently under development by the same authors, and would be the perfect candidate architecture for flutter active control.

5 Conclusions

The main objective of the *In.A.Team* group at Politecnico di Torino, Italy is the development of simple analytical methods which can be used for estimation of main factors contributing to the occurrence of different critical and supercritical behaviour of next generation of innovative aircrafts. A range of structural models for aeroelastic analysis of composite high aspect ratio wing configurations are discussed in this paper and proposed for a subsequent control systems design. A simple 3 D.o.F aero-servo-elastic model has been introduced and classical open loop flutter velocity is determined according to Goland's wing case.

A linear quadratic regulator (LQR) control strategy has been tested and some limits have been highlighted especially in presence of gradually or instantaneous degradation of the structural bending stiffness.

The preliminary analysis shows how the introduction of an adaptive control system could be a preferred solution when the system becomes very sensitive to model parameter uncertainties. A preliminary architecture of the advanced control strategy is presented as a basis for future development.

References

[1] M. J. Patil and D. H. Hodges. Flight dynamics of highly flexible flying wings. Journal of Aircraft, 43(6):1790–1799, 2006.

[2] Tuzcu I; Marzocca P; Cestino E; Romeo G; Frulla G. "Stability and Control of a High-Altitude-Long-Endurance UAV", Journal Of Guidance Control and Dynamics, 30 (3): 713-72, 2007

[3] Romeo, G., Frulla, G., Cestino, E., Marzocca, P., Tuzcu, I. "Nonlinear Aeroelastic Modelling and Experiments of Flexible Wings," Proc. of 47th AIAA/ASME/ASCE/AHS/ASC Structures, Structural Dynamics, Materials Conference, Newport RI, 1-4 May, 2006.

[4] Romeo G; Frulla G; Cestino E.; Marzocca P, "Non-linear Aeroelastic Behavior of Highly Flexible HALE Wings", Proceedings 25th ICAS Congress, Hamburg Germany 3-8 September, 2006.

[5] G. Frulla, E. Cestino, P. Marzocca "Critical behaviour of slender wing configurations" Proc. of the institution of mechanical engineers. Part G, Journal of Aerospace Engineering Vol.224 pp.527-636 2010.

[6] C. E. S. Cesnik and W. Su, "Nonlinear aeroelastic modeling and analysis of fully flexible aircraft", 46th AIAA/ASME/ASCE/AHS/ASC Structures, Structural Dynamics and Materials Conference, 7, April 2005.

[7] Thomas E. Noll, John M. Brown et Al., "Investigation of the Helios Prototype Aircraft Mishap", Vol.1, January 2004.

[8] Bispringhoff, R., Ashley, H., and Halfman, R., "Aeroelasticity", 1955 (Dover, New York).

[9] Lee, B.H.K., Price, S.J., Wong, Y.S. "Nonlinear Aeroelastic Analysis of Airfoils: Bifurcation and Chaos", Progress in Aerospace Sciences, 1999, 35 (3), 205–334.

[10] Tang, D .M ., Dowell, E.H. "Comments on The Onera Stall Aerodynamic Model and its Impact on Aeroelastic Stability", Journal of Fluids and Structures,1996, 10, 353 – 366.

[11] Borello F., Cestino E., Frulla G., Structural "Uncertainity Effect on Classical Wing Flutter Characteristics", Journal of Aerospace Engineering 2010, DOI: 10.1061/(ASCE)AS.1943-5525.0000049.

[12] Beddoes T., "A synthesis of unsteady aerodynamic effects including stall hysteresis", Vertica 1:22, 113-123, 1976.

[13] Leishman J., Beddoes T., "A semi-empirical model for dynamic stall", J Am Helicopter Soc 1989;34:3–17

[14] Nayfeh, A.H., Pai, P.F., "Linear and Non-linear Structural Mechanics", 2004 (Wiley Interscience, New York).

[15] Hodges, D.H., Dowell, E.H., "Nonlinear Equations of Motion for the Elastic Bending and Torsion of Twisted Non Uniform Rotor Blades", NASA TN D-7818, 1974.

[16] Crespo da Silva, M.R.M., Glynn, C.C., "Nonlinear Flexural-Flexural-Torsional Dynamics of Inextensional Beams. Equations of Motion", Journal of Structural Mechanics, 1978, 6(4), 437-448.

[17] Cestino E., Frulla G., "Critical Aeroelastic Behaviour Of Slender Composite Wings In An Incompressible Flow, Composite Materials in Engineering Structures", ©2010 Nova Science Publishers, Inc. ISBN: 978-1-61728-857-9.

[18] Berdichevsky V., Armanios E.A. , Badir, A.M. "Theory of Anisotropic Thin-Walled closed-cross-section Beams". Composites Engineering. Vol. 2, no.5-7, 1992, pp.411-432.

[19] Armanios E.A., Badir, A.M., "Free Vibration Analysis of Anisotropic Thin-walled Closed-Section Beams" . AIAA Journal Vol. 33, No. 10 , October 1995. pp. 1905-1910.

[20] Roger K.L., "Airplane Math Modeling Methods for Active Control Design", AGARD Report 228,1977.
[21] Kim T., Nam C. and Kim Y., "Reduced-order aeroservoelastic model with an unsteady aerodynamic eigenformulation", AIAA Journal 35 (1997), pp. 1087–1088.
[22] Goland, M. "The Flutter of a Uniform Cantilever Wing, Journal of Applied Mechanics", 1945, 12 (4), 197-208.
[23] Heeg J., "Analytical and experimental investigation of flutter suppression by piezoelectric actuation" NASA Technical Paper no. 3241, USA; 1993.
[24] J. Rocha, P. Moniz and A. Suleman, "Aeroelastic Control of a Wing with Active Skins Using Piezoelectric Patches", Mechanics of Advanced Materials and Structures, 14:23–32, 2007.
[25] Irene M. Gregory, Chengyu Cao, Vijay V. Patel. and Naira Hovakimyan, "Adaptive Control Laws for Flexible Semi-Span Wind Tunnel Model of High-Aspect Ratio Flying Wing", AIAA Guidance, Navigation and Control Conference and Exhibit, 20-23 August 2007, Hilton Head, South Carolina, AIAA 2007-6525.
[26] Z. Zang, R. Bitmead, "Transient Bounds for Adaptive Control Systems", Proceedings of 29th IEEE Conference on Decision and Control, pp. 2724-2729, Honolulu, HI, December 1990.
[27] C. Cao, N. Hovakimyan, "Design and analysis of a novel L1 Adaptive controller, Part 1: Control signal and asymptotic stability", Proceedings of the 2006 American Control Conference, Minneapolis, Minnesota, USA, June 14-16, 2006.
[28] C. Cao, N. Hovakimyan, "Design and analysis of a novel L1 Adaptive controller, Part 2: Guaranteed Transient Performance", Proceedings of the 2006 American Control Conference, Minneapolis, Minnesota, USA, June 14-16, 2006.
[29] H.K.Khalil, "Nonlinear Systems", Prentice Hall, New Jersey, 2002.
[30] E.Xargay, N.Hovakimyan, C.Cao, "$\mathcal{L}_1$ adaptive controller for MIMO systems in the presence of nonlinear unmatched uncertainties", 2010 American Control Conference, June 30-July 02, 2010, Baltimore, MD.

Contact Author Email Address

In alphabetical order:
manuela.battipede@polito.it
enrico.cestino@polito.it
giacomo.frulla@polito.it
stefano.gerussi@gmail.com
piero.gili@polito.it

Copyright Statement